Supporting Information

Hill et al. 10.1073/pnas.1001229107

SI Text

Cortical thickness is another measure that may be relevant to understanding the pattern of postnatal cortical expansion. In principle, regions of high expansion might reflect cortex that expanded in surface area preferentially instead of increasing in thickness and vice versa. However, this does not fit well with adult thickness data. For example, high-expanding regions (lateral temporal cortex, temporal pole, and precentral gyrus) are among the thickest regions (3.5–4.5 mm), whereas the low-expanding visual cortex is one of the thinnest (≈2 mm) (1, 2). Thus, to a first approximation, regions of high postnatal expansion tend to be thickest in adults and vice versa. The correlation is imperfect; noteworthy exceptions include the low-expanding medial temporal and medial parietal cortices that are relatively thick (≈3 mm) in adults, and the high-expanding dorsal frontal cortex that is relatively thin (≈2.5 mm) (3, 4). To address this issue fully, it is critical to know the distribution of cortical thickness at birth. This is difficult to accurately discern from in vivo MRI datasets because of inadequate resolution in term infants. Histological atlases of term infant cortical structure suggest that, as in adults, cortical thickness varies regionally across the cortex following a similar pattern. Specifically, the term infant visual cortex is relatively thin (≈1 mm) and the precentral gyrus is relatively thick (≈1.5 mm) as in adults (5).

SI Materials and Methods

Cortical Surface Reconstruction. High resolution, T2-weighted and T1-weighted MRI scans were obtained for term infant and adult subjects, respectively (Fig. S1*A*). All infant MRIs were aligned to the anterior commissure–posterior commissure (AC–PC) orientation and origin by rigid body translation and rotation using Caret software (http://brainvis.wustl.edu) (6). Adult MRI volumes were registered to the Washington University 711–2C version of stereotaxic atlas space. Each brain was cropped along the midline for separate processing of left and right hemispheres. Midcortical (cortical layer IV) segmentation volumes were generated for term infants and adults using the semiautomated LIGASE and SureFit methods, respectively (Fig. S1*B*). Aiming for the cortical midthickness has the advantage that each square millimeter of surface area represents approximately the same cortical volume irrespective of gyral or sulcal location (7).

Cortical surface reconstructions were generated for each hemisphere using tools in Caret. A raw surface was generated by a tessellation running along the boundary of the segmentation volume and smoothed slightly to generate a 3D "fiducial" surface (Fig. S1*C*). A closed contour along the boundary of cortex with the corpus callosum, basal forebrain, and the fundus of the parahippocampal fissure, designated the noncortical medial wall, was manually delineated in Caret (Fig. S1*C*, medial view). An inflated configuration was generated by applying 300 iterations of inflation to the fiducial surface (Fig. S3*A*). A spherical surface (Fig. S3*B*), used for registration, was also generated for each surface.

Atlas Construction and Registration. ***Target atlas generation.*** To quantitatively compare term infant and adult populations without bias toward either age group, a hybrid atlas target was created that reflects the average shape characteristics of both age groups. The hybrid atlas is denoted as the PALS-TA24 atlas because it is a PALS atlas derived from a total of 24 term and adult hemispheres. A conceptual illustration of the approach toward atlas generation adopted in this study is illustrated in Fig. S2.

Generation of the PALS-TA24 involved three main stages: (*i*) delineating landmarks on each individual hemisphere; (*ii*) generating population-average landmarks to serve as the target for registration; and (*iii*) registering each individual to the "standard mesh" (73,730-node) atlas sphere and generating standard mesh representations of each individual fiducial surface.

Delineating registration landmarks. A set of six landmarks ("Core six") that are highly consistent in both term infants and adults (7, 8) was delineated on each individual fiducial surface. Figure S3 *A* and *B* shows examples of these six landmarks displayed on inflated and spherical surfaces of an individual term infant.

Population-average set of landmarks (atlas). The population-average landmarks that served as the target for registration were generated in two stages. A target spherical surface was created using a standard-mesh 73,730 node sphere (Fig. S3 *C–E*), the surface area of which was scaled to the average surface area of all 24 (term infant and adult) right hemisphere native mesh spherical surface maps described above. Corresponding landmarks from each individual's native mesh spherical surface were averaged together (after mirror-reflecting the left hemisphere landmarks) and projected to the standard-mesh target sphere. Individual variability in these landmarks is modest, and the choice of individuals should have only a small effect on the average contour of each landmark (Fig. S3*C*). As expected, there were modest differences in the average trajectory for each age group (Fig. S3*D*), thus supporting the use of a combined target reflecting shape characteristics of both populations (Fig. S3*E*).

Registering individuals to PALS-TA24 atlas. Each hemisphere was registered to the target atlas using a spherical registration algorithm (7). Briefly, the algorithm uses multiple cycles of landmark-constrained smoothing coupled with shape-preserving morphing iterations that reduce local linear and angular distortions (9, 10). After registration, each individual hemisphere was resampled to the standard-mesh tessellation, thereby establishing node-to-node correspondences among all individuals.

Interatlas surface-based registration. To map population data from the PALS-B12 atlas (7) to the PALS-TA24 atlas, an interatlas registration was carried out. For the right hemisphere, an average "B12" fiducial surface was created in PALS-TA24 space by averaging all 12 standard-mesh right hemisphere adult fiducial surfaces. A total of 22 registration landmarks were drawn on the average "B12" fiducial surface in PALS-TA24 space and registered to a corresponding set of landmarks previously established on the average "B12" fiducial surface in PALS-B12 space (8) to generate a right-hemisphere mapping between atlases. This mapping was used to register Brodmann areas, a surface atlas of the macaque monkey, and a map of evolutionary surface expansion generated in PALS-B12 space to the PALS-TA24 atlas.

Scale normalization. The adult anatomical MRI volumes for the PALS-B12 atlas had been registered to Washington University's 711–2C template by affine transformation before segmentation (7, 11), whereas the term infant anatomic MRI volumes had not (8). To control for this methodological difference and to obtain a set of surfaces as comparable as possible for between group analyses, each fiducial surface was normalized to the age-specific population average surface dimensions, as previously described (8).

1. Fischl B, Dale AM (2000) Measuring the thickness of the human cerebral cortex from magnetic resonance images. *Proc Natl Acad Sci USA* 97:11050–11055.

2. Hutton C, De Vita E, Ashburner J, Deichmann R, Turner R (2008) Voxel-based cortical thickness measurements in MRI. *Neuroimage* 40:1701–1710.

3. Burggren AC, et al. (2008) Reduced cortical thickness in hippocampal subregions among cognitively normal apolipoprotein E e4 carriers. *Neuroimage* 41:1177–1183.
4. Venkatasubramanian G, Jayakumar PN, Gangadhar BN, Keshavan MS (2008) Automated MRI parcellation study of regional volume and thickness of prefrontal cortex (PFC) in antipsychotic-naive schizophrenia. *Acta Psychiatr Scand* 117:420–431.
5. Bayer SA, Altman J (2003) *The Human Brain during the Third Trimester* (CRC Press, Boca Raton).
6. Van Essen DC, et al. (2001) An integrated software suite for surface-based analyses of cerebral cortex. *J Am Med Inform Assoc* 8:443–459.
7. Van Essen DC (2005) A population-average, landmark- and surface-based (PALS) atlas of human cerebral cortex. *Neuroimage* 28:635–662.
8. Hill J, et al. (2010) A surface-based analysis of hemispheric asymmetries and folding of cerebral cortex in term-born human infants. *J Neurosci* 30:2268–2276.
9. Van Essen DC, et al. (2001) Mapping visual cortex in monkeys and humans using surface-based atlases. *Vision Res* 41:1359–1378.
10. Van Essen DC (2004) Surface-based approaches to spatial localization and registration in primate cerebral cortex. *Neuroimage* 23 (Suppl 1):S97–S107.
11. Buckner RL, et al. (2004) A unified approach for morphometric and functional data analysis in young, old, and demented adults using automated atlas-based head size normalization: Reliability and validation against manual measurement of total intracranial volume. *Neuroimage* 23:724–738.

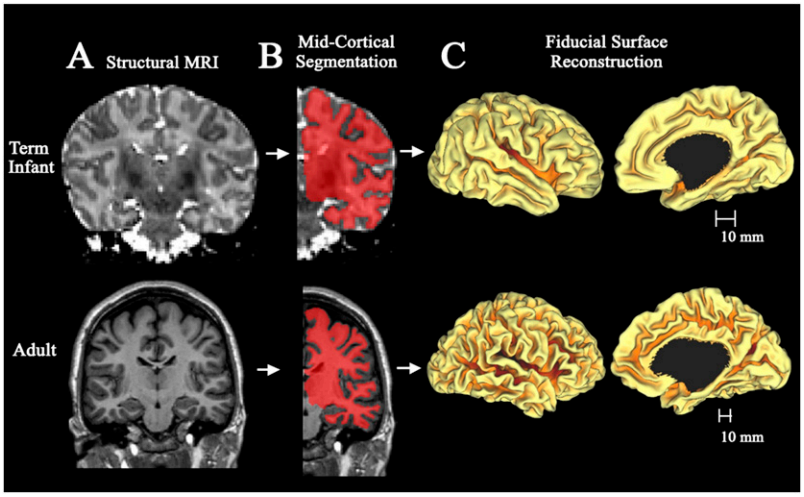

Fig. S1. Generation of cortical surface reconstructions for a term infant (top) and adult (bottom). (*A*) Example of a T2-weighted (term infant) and T1-weighted (adult) structural MRI volume. (*B*) Right hemisphere midcortical segmentation volume overlaid on the structural MRI volume. (*C*) Lateral (*Left*) and medial (*Right*) views of the fiducial surface reconstruction. Noncortical medial wall has been manually smoothed and blackened out.

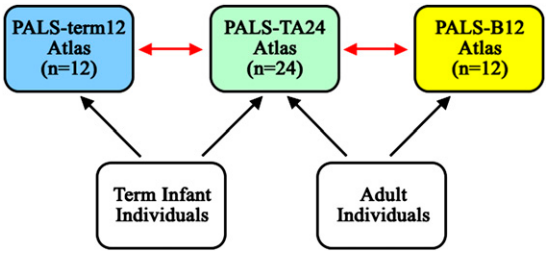

Fig. S2. Conceptual framework for the PALS atlas approach. White boxes represent individuals in their native space; colored boxes represent distinct population average atlases as labeled. Black arrows indicate registration of individuals to distinct atlases; red arrows indicate interatlas registration. PALS-TA24 atlas target reflects the average shape characteristics of both term infants and adults.

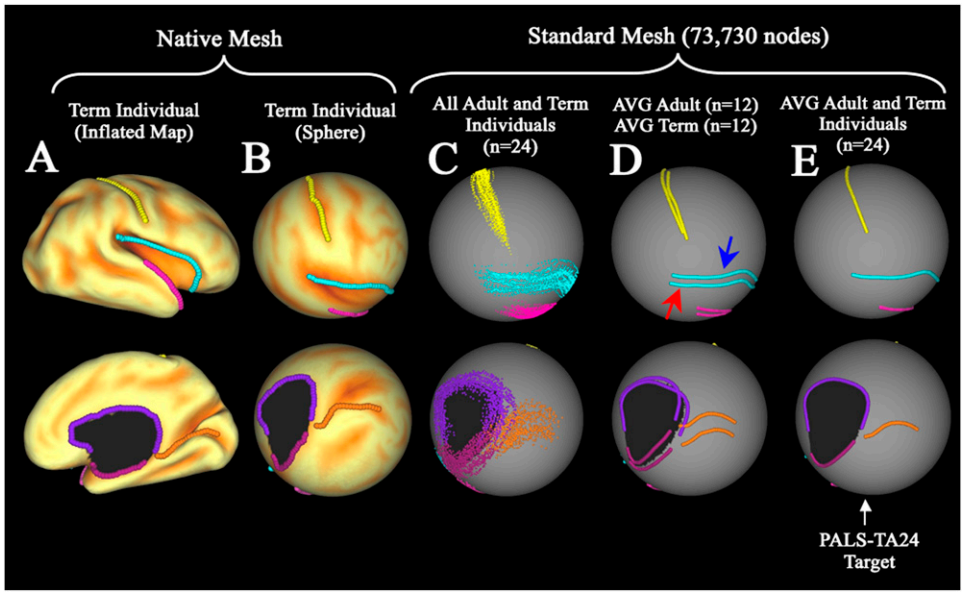

Fig. S3. Registration landmarks and creation of PALS-TA24 registration target. Individual, population, and population-average landmarks are shown on several surfaces. Lateral views are displayed in the top row and medial views in the bottom row. (*A*) Native mesh inflated surface configuration for one term infant individual overlaid with a map of sulcal depth. The six landmarks (Core 6) used for registration are displayed on the surface. On the lateral surface, these include the fundus of the central sulcus (yellow), Sylvian fissure (blue), and anterior half of the superior temporal gyrus (pink). Medial landmarks include the calcarine sulcus (orange) and the cortical margin of the medial wall divided into dorsal (purple) and ventral (magenta) portions. (*B*) Core 6 landmarks displayed on native mesh spherical surface map for the same individual overlaid with a map of sulcal depth. (*C*) Core 6 landmarks from both hemispheres (right and mirror-flipped left) of all 24 term infant and adult individuals projected to the standard mesh (73,730 node) PALS-TA24 spherical map. (*D*) Average border trajectory of each landmark for the 12 adult and 12 term infant individuals separately displayed on standard mesh sphere. For Sylvian fissure landmark, blue arrow denotes the average adult landmark, and red arrow denotes the average term infant landmark. Average term infant landmarks serve as the target for the PALS-term12 atlas; average adult landmarks serve as the target for the PALS-B12 atlas. (*E*) Average border trajectory of each landmark for all 24 term infant and adult individuals displayed on the standard mesh spherical map. These average landmarks served as the target for surface based registration to the PALS-TA24 atlas.